Surface and Adsorption Properties of Activated Carbon Fabric Prepared from Cellulosic Polymer: Mixed Activation Method

Surendra Bhati,[*] **J. S. Mahur, Savita Dixit,**[†] **and O. N. Choubey**

Department of chemistry, Govt. Narmada P.G. College, Barkatullah.Universtity, M.P., India -461001
[*]*E-mail: surendrabhati04@gmail.com*
[†]*Department of applied chemistry, Maulana Azad National Institute of Technology, M.P., India -462016*

In this study, activated carbon fabric was prepared from a cellulose-based polymer (viscose rayon) via a combination of physical and chemical activation (mixed activation) processes by means of CO_2 as a gasifying agent and surface and adsorption properties were evaluated. Experiments were performed to investigate the consequence of activation temperature (750, 800, 850 and 925 °C), activation time (15, 30, 45 and 60 minutes) and CO_2 flow rate (100, 200, 300 and 400 mL/min) on the surface and adsorption properties of ACF. The nitrogen adsorption isotherm at 77 K was measured and used for the determination of surface area, total pore volume, micropore volume, mesopore volume and pore size distribution using BET, *t*-plot, DR, BJH and DFT methods, respectively. It was observed that BET surface area and TPV increase with rising activation temperature and time due to the formation of new pores and the alteration of micropores into mesopores. It was also found that activation temperature dominantly affects the surface properties of ACF. The adsorption of iodine and CCl_4 onto ACF was investigated and both were found to correlate with surface area.

Key Words : Activated carbon fabric, BET surface area, Microporosity, Pore size distribution

Introduction

Now a day, there is broad interest in the use of activated carbons or porous carbons as adsorbent to remove toxic chemicals and gases from air and water due to its adsorption capacities.[1-3] Mainly four types of activated carbons, divided on the basis of size and shape, are available in market; granular (GAC), powder (PAC), spherical (ACS) and fiber (ACFs). Out of them the ACFs increasing attention due to its superiority over other forms.[4] It has a high surface area, is lightweight, has a smaller fiber diameter (which minimizes diffusion limitations), low pressure drop, easy regeneration, easy accessibility to micropores and narrow pore size distribution. It can be fabricated into cloth, felt, and paper and has great adsorption capacity for low concentrations of adsorbates.[5,6]

Since the 1970s, many types of synthetic and natural fibers has been used as precursors for fibrous activated carbon like polyacrylonitrile (PAN),[7] polyphenol, viscose rayon,[8,9] cellulose phosphate, phenolic,[10,11] and pitch based fibers.[12,13] Out of them, cellulosic polymer such as cotton, rayon and jute was more than ever focused, for the reason that of their low cost, commercial availability of precursor, high microporosity of prepared activated carbons and biodegradability of precursor. The Physical and chemical activation is a well established method for the preparation of activated carbons fiber.[14-16] In the physical activation, the precursor material is activated in presence of oxidizing atmosphere while in chemical activation the precursor is first impregnated with flame retardant reagent (*i.e.* Lewis acids) and then subjected to heat treatment under inert atmosphere. Some researcher has been used combination of both the techniques known as "mixed activation" but their study was not well focused.[17-19] It is well known that high surface area, pore volumes and percent microporosity ($P_{micro.}$) of activated carbons are key characteristics which decide the use of the activated carbon for different applications. The final property of activated carbon depends upon the activation parameters.[20,21] Flame retardant reagent and flow rate of the reacting gas also play significant role in the development of pores in activated carbon.[22] Kyotani (2000) summarized the parameters that control the pore structure, but uncertainty remains as such in our understanding of which factors control what factor in the preparation of activated carbons.[23]

In this study, viscose rayon knitted fabric was taken as raw material for the preparation of activated carbon fabric (ACF). Using mixed activation method, the effect of activation temperature, activation time and CO_2 gas flow rate on the surface and adsorption properties of ACF was identified. The TGA, proximate and ultimate analysis and surface analysis were also studied.

Experimental

Materials and Methods. A viscose rayon knitted fabric having 280-300 g/m² was used as the precursor for the preparation of activated carbon fabric. Analytical grade *Ortho*-Phosphoric acid of about 85% pure (Chemical Formula = H_3PO_4, Mol. wt. = 98) was purchased from Merck specialties private Ltd. (Mumbai, India). Carbon dioxide was procured locally and was purified using a purification system (Analab, Gujrat, India) to remove any moisture and organic impurities.

The series of ACF samples were prepared using mixed activation under different experimental conditions. In this method, ACF was prepared using 2 steps: (i) strips (15 × 15 cm^2) of viscose rayon fabrics were immersed in an aqueous solution of a flame retardant reagent (H_3PO_4) of concentration 5% for 1hr at a temperature of 70 °C. The immersed samples were drained and dried in a hot air oven at temperature of 85 °C for 3 hours. (ii) The dried strips were then heat treated under the flow of nitrogen and then activated at different temperature for different time under CO_2 atmosphere, in high temperature programmable tubular furnace with dimensions of 45 × 20 cm^2 (length × width) consisting of a SS reactor of dimensions 100 × 120 mm^2 (length × width).

Characterization. Thermal degradation of the viscose rayon fabric (VF) and the phosphoric acid treated fabric "Pretreated fabric (PF)" was performed using a Diamond TG/DTA instrument (Perkin Elmer). The TGA curves were obtained under a N_2 atmosphere at a flow rate of 200 mL/ min and a scanning rate of 10 °C/min.

The Proximate analysis was performed according to American Standard of Testing and Methods (ASTM-D 3172-3175, 2010) and the results obtained were expressed in terms of moisture content, ash content, and volatile matter. To determine moisture content, 1 gm samples of each VF, PF, and ACF were taken in different crucibles and heated to 110 °C in an oven until complete dehydration was obtained. The samples were then decomposed in a furnace at 950 °C for 6 min to determine volatile matter. Approximately, 1 gm of each sample was placed in covered crucibles and heated up to 750 °C for 3 h in a muffle furnace to determine the ash content. The ultimate analyses of these samples were examined using a CHNS/O analyzer (Perkin Elmer series II, 2400). The oxygen content was determined by subtracting the C, H and N contents from the total.

A Quantachrome Autosorb-1, surface area analyzer was used to determine the N_2 adsorption isotherm at 77 K, which is used to calculate the surface area and pore volumes of ACF samples. The ACF samples were degassed for 3 h under vacuum at 150 °C prior to experiment under nitrogen. The BET surface area (S_{BET}), total pore volume (TPV), micropore volume (V_{micro}), mesopore volume (V_{meso}), and pore size distribution (PSD) of the ACF were calculated using the BET (Brunauer Emmett & Teller) equation, *t*-plot, DR (Dubinin-Radushkovich), BJH (Barett, Joyner & Halenda) and DFT (Density Functional Theory) methods, respectively. A Jeol (Model-6510) make scanning electron microscope was used to study the morphological structure of prepared activated carbon fabrics.

Results and Discussions

Thermal Degradation Behavior. Figure 1 shows the weight loss of viscose rayon fabric (VF) and pretreated fabric (PF) with respect to increasing temperature. Initially, the weight loss of VF and PF was 7.5% and 8.5%, respectively, at 200 °C. This was due to the removal of moisture and some volatile matter. The drastic weight loss of 72.1% for VF and
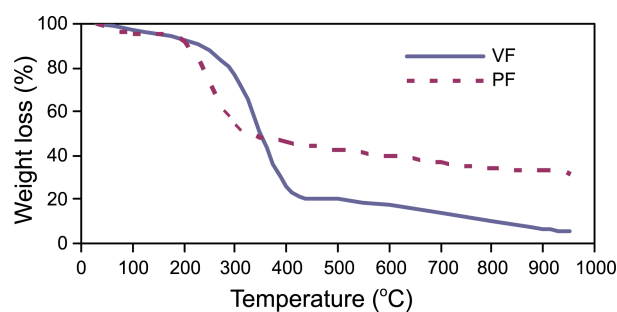

Figure 1. Thermograph of VF (Viscose rayon fabric) and PF (Pretreated fabric).

47.2% for PF were observed between 200-500 °C; however, beyond 500 °C the weight loss decreased for PF. At 950 °C a maximum yield of 5.5% for VF and 31.9% for PF was obtained. The phosphoric acid works as catalyst to decrease the thermal degradation temperature (≈ 250 °C) and leads to the higher char yield then to VF.

The thermal degradation of VF is always linked with dehydration and depolymerization with high activation energies. To conquer this energy, a very high temperature must be supplied to break the C-OH, C-H and C-O-C bonds in the cellulosic molecules. Once the significant temperature is attained, the thermal degradation occur, but in an uncontrolled manner, resulting in the formation of L-glucosan and flammable materials, causing an extremely low yield.

Adsorption Isotherm at 77 K. The adsorption isotherm indicates the specific volume adsorbed by the sample as a function of relative pressure (P/P^0) at constant temperature. Figure 2 shows the adsorption isotherm for ACF produced at different activation temperature at constant gas flow (200 mL/min) and activation time (60 minute). It has been seen that, most of ACF samples exhibit a Type-I isotherm with majority of the adsorption at a lower relative pressure range indicating the micro porous nature of the sample; however ACF-925/60/200 shows small adsorption at higher relative pressure indicating the presence of some mesopores.

Effect of Activation Temperature. The results of effect of activation temperature on surface properties of ACF are summarized in Table 1. As shown in Table 1, when the
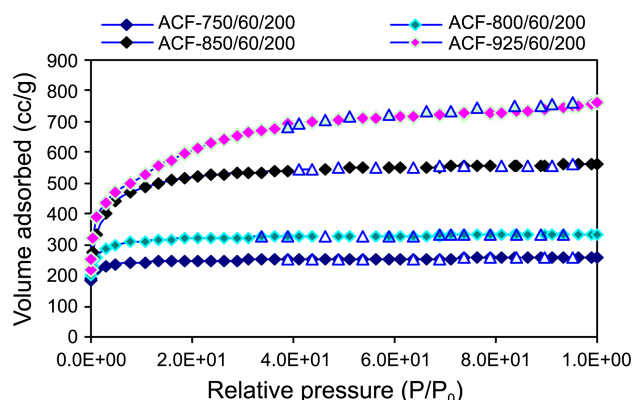

Figure 2. Adsorption isotherms at 77 K for ACF (Where, □ = Adsorption and △ = Desorption).

Table 1. Surface properties of Activated Carbon Fabric

Sample [a]ACF-X/Y/Z	Yield (%)	S_{BET} (m²/g)	TPV (cc/g)	DR-$V_{micro.}$ (cc/g)	$P_{micro.}$ (%)	BJH $V_{meso.}$ (cc/g)	Average Pore Dia. (Å)
ACF-925/60/200	8	2097	1.13	0.72	63.7	0.41	22.1
ACF-850/60/100	17.5	1880	0.81	0.63	77.8	0.09	18.5
ACF-850/60/200	15.2	1964	0.87	0.69	79.3	0.14	18.7
ACF-850/60/300	12.4	2088	1.02	0.77	75.5	0.31	19.2
ACF-850/60/400	11.5	2199	1.24	0.84	67.7	0.41	19.8
ACF-850/45/200	16.5	1606	0.75	0.64	85.3	0.09	18.2
ACF-850/30/200	20.3	1402	0.61	0.51	83.6	0.04	17.5
ACF-850/15/200	20.7	1254	0.55	0.44	80.0	0.04	17.2
ACF-800/60/200	23.2	1225	0.52	0.48	92.3	0.03	16.8
ACF-750/60/200	26.3	985	0.32	0.31	96.9	0.01	15.4

[a](ACF-X/Y/Z) Where X = activation temperature, Y = activation time and Z = CO_2 gas flow rate

temperature was increased from 750 to 925 °C, the S_{BET} increased from 985 to 2097 m²/g but the yield of the ACF decreased from 26.3% to 8%; this was due to the reaction between the carbon of the precursor and the CO_2 gas, resulting CO gas formation.

As temperature increased, the TPV and V_{meso} also increased, possibly due to the broadening of pores due to the gasification reactions, which is enhanced at high temperature. From Figure 3(a), it was observed that after 850 °C the S_{BET} increased very slowly while the P_{micro} decreased abruptly, indicates the formation of larger size pores due to faster gasification reaction. Figure 3(b), shows the PSD of the ACF samples. It was observed that the pores of size < 10 Å decreased and 10-15 and 15-20 Å pores increased on increasing the activation temperature due to widening of pores. From literature review it has been conclude that, the activation temperature mainly affects the surface properties of activated carbons. It was also observed from the Table 1
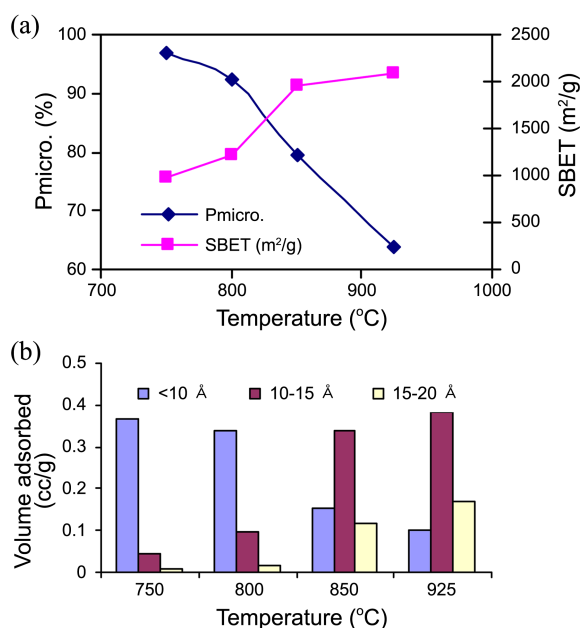
that the V_{micro} increases faster up to 850 °C and thereafter becomes slow or relatively constant due to conversion of smaller pores into larger pores or development of large size pores. As shown in Table 1, the average pore diameter of all the ACF samples was smaller then 20 Å that revealed that the ACF composed of micropore and mesopores not macropores.

Effect of Activation Time. The effect of activation time on the surface properties of ACF are summarized in Table 1. As shown in Table 1, when the activation time was increased from 15 to 60 min, the S_{BET} and V_{micro} increased and reached a maximum (1964 m²/g) at 60 min, indicating that 60 min is the optimum time to produce ACF with a high surface area under the given sets of conditions.

As shown in Figure 4(a), the P_{micro} was initially increased with an increase in activation time from 15 to 30 min. and reaches a maximum value at 30 min (85.3%). It then starts to decrease and reaches 80.0% at 60 min due to faster gasifi-
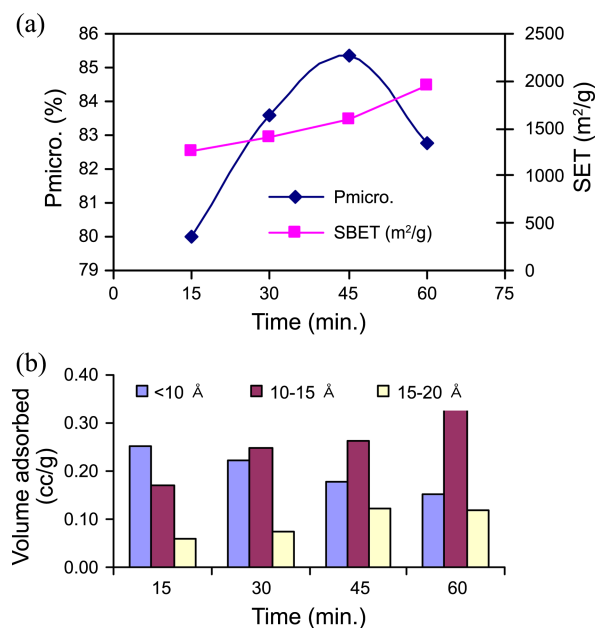

Figure 3. Effect of activation temperature, (a) Microporsity and SBET, (b) Pore size distribution & pore volume. (Activation time = 60 minute, CO_2 flow rate = 200 mL/minute)

Figure 4. Effect of activation time, (a) Microporsity and S_{BET}, (b) Pore size distribution & Pore volume. (Activation temperature = 850 °C, CO_2 flow rate = 200 mL/minute)

cation. The TPV and V_{micro} were increased with an increased in activation time from 0.53 to 0.96 and from 0.44 to 0.69 cc/g, respectively. Figure 4 (B), shows the PSD of the ACF samples. It can be seen that the activation time does not affects the PSD much more; however the average pore diameter is increase from 17.7 to 18.7 Å on increasing activation time.

Effect of CO_2 Flow Rate. As shown in the Table 1, the SBET was increased on increasing CO_2 flow from 100 to 400 mL/minute and reached a maximum (2199 m²/g). It has been also observed from the Table 1 that on increasing the flow rate yield of ACF decreased from 17.5% to 11.5% and TPV and V_{micro} increased from, 0.89 cc/g to 1.24 cc/g and 0.63 cc/g to 0.84 cc/g, respectively. As shown in Figure 5(a), V_{meso} and P_{micro} were increased with increased in gas flow rate from 100 to 200 mL/min thereafter decreased, indicating that 200 mL/min is the optimum flow to get high micro-porosity at 850 °C with 60 min of activation time. Figure 5(b) data indicates that the CO_2 gas flow rate very little affects the PSD of ACF samples; however the average pore size increased from 18.5 to 19.8 Å on increasing flow rate.

Morphology of ACF. Figure 6(a, b & c) displays the scanning electron microscope (SEM) images of viscose-based ACF. Figure 6(a), at 30X magnification illustrate the fabric integrity with rough surface obtained after the activation process and the knitting pattern of the ACF-850/60/200 fabric; Figure 6(b & c) shows the broken fiber in ACF-925/60/200 sample, indicating the severity of the activation condition aided by high activation temperature. Figure 6(c), also shows the morphology of individual fiber with blunt edges indicating the presence of viscose rayon fiber. The SEM images of other samples are not shown since all samples
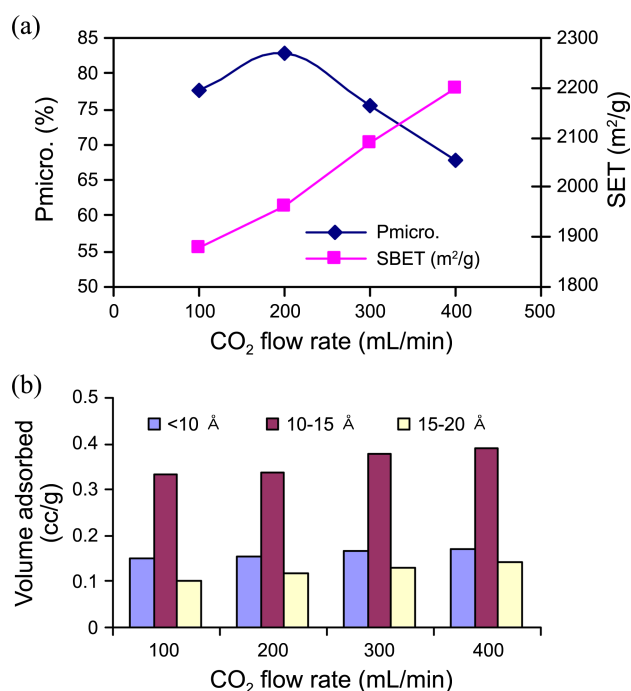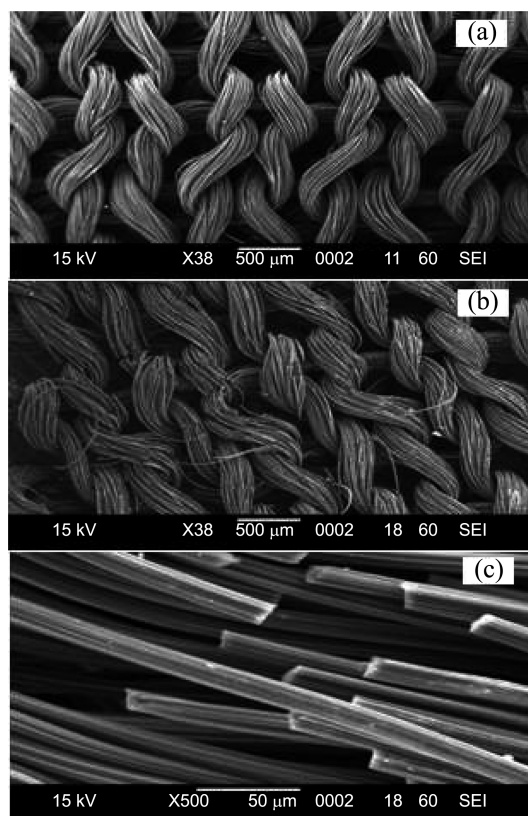

Figure 6. SEM images of ACF (Where, (a) = ACF-850/60/200 (no broken fibers), (b) = ACF-925/60/200 (broken fiber), (c) = magnified image of ACF-925/60/200).

have the same morphology.

Proximate and Ultimate Analysis. Table 2 shows the results of proximate and ultimate analysis of VF, PF and ACF-850/60/200. The VF is rich in carbon (44.5%) and has low ash content (0.2%). The carbon percentages show incremental increase up to 81.9% after activation while oxygen and hydrogen show gradual reduction to 14.5% and 1.1%, respectively. This is due to the removal of volatile and non-volatile matter during the carbonization and activation process. The PF sample shows 5.1% phosphors content, it is present in oxides forms; however, phosphorous absent in the ACF sample because the remaining phosphorous removed

Figure 5. Effect of CO_2 flow rate, (a) Microporsity and S_{BET}, (b) Pore size distribution & Pore volume. (Activation temperature = 850 °C, Activation time = 60 minutes)

Table 2. Proximate and ultimate analysis of VF, PF & ACF

	VF	PF	ACF 850/60/200
Proximate analysis			
Moisture	6.5	5.9	0.4
Volatile matter	86.8	72.5	3.2
Ash	0.2	2.4	0.04
Ultimate analysis			
Carbon	44.5	30.8	81.9
Hydrogen	6.25	5.6	1.1
Nitrogen	0.2	0.2	0.2
Oxygen	49.3	63.4	14.5
Phosphorus	0	5.1	0

Cellulose Based Activated Carbon Fabric

Bull. Korean Chem. Soc. **2013**, Vol. 34, No. 2 573
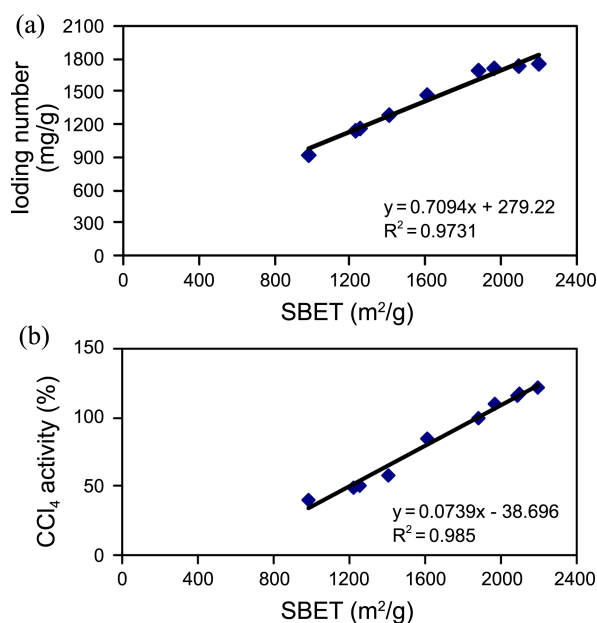

Figure 7. Correlation between, (a) = Iodine Number with S_{BET}, (b) = CCl_4 activity (%) with S_{BET}.

during washing after activation. The VF sample also shows non removable, small amount of N, which may include during its preparation.

Iodine and CCl_4 Adsorption. Iodine and CCl_4 adsorption capacity of prepared ACF was determined using the American standard Testing and Method (ASTM-D46078-94) and desiccator method, respectively.

The iodine adsorption represents as iodine number; it is defined as the milligram of iodine adsorbed by one gram of carbon when the iodine concentration of the residual filtrate is 0.02 N. The adsorption capacity of any adsorbent is dependent on the concentration of the adsorbent in the medium in contact with the carbon. Thus, the concentration of the residual filtrate must be specified or known so those appropriate factors may be applied to correct the concentration to agree with the definition. The higher iodine number and high CCl_4 adsorption indicates higher microporosity as well as higher surface area. It was observed from Figure 7(a) & 7(b) that the iodine number and CCl_4 adsorption shows linear relationship with S_{BET} with correlation coefficient (R) of 0.9731 & 0.985, respectively. From both of these relations, it is clear that as S_{BET} increases, the adsorption capacities of activated carbon samples also increase.

Conclusion

In summary, a series of viscose rayon-based ACF were prepared using a mixed activation method taking CO_2 as a gasifying agent. The study revealed that the activation temperature largely influences the surface area, V_{micro}, V_{meso} and PSD of ACF. The S_{BET} and micropore volume of the activated samples increased from 985 m^2/g to 2097 m^2/g and

0.31 cc/g to 0.72 cc/g, respectively, with an increase in activation temperature. On the other hand, the P_{micro} of the samples continuously decreased due to the conversion of micropores to mesopores. Activation of viscose rayon fabric at 850 °C for 15 to 60 minutes of activation time was found to increase the S_{BET} and V_{micro} from 1254 to 1964 m^2/g and 0.44 to 0.72 cc/g, respectively. There was an increase in P_{micro} up to 45 minutes followed by decrease in microporosity, indicating the conversion of micropore into mesopore. A small increase in S_{BET} and TPV was observed after increasing the gas flow rate during activation from 100 to 400 mL/min.

References

1. Debasish, D.; Vivekanand, G.; Nishith, V. *Carbon* **2004**, *42*, 6409.
2. Vivekanand, G.; Ashutosh, S.; Nishith, V. *Chemical Engineering and Processing* **2006**, *45*, 1.
3. Brasquet, C.; Cloirec, P. Le *Carbon* **1997**, *35*, 1307.
4. Sadamura, H.; Kobayashi, S.; Honda, S.; Suzuki, N. *et al. Electrochemistry* **2000**, *68*(5), 321.
5. Dimotakis, E.; Cal, M. P.; Economy, J.; Rood, M. J.; Larson, S. M. *Environ Science Technology* **1995**, *29*, 1876.
6. Cal, M. P.; Rood, M. J.; Larson, S. M. *Energy and Fuels* **1997**, *11*(2), 311.
7. Shimazaki, K.; Ogawa, H. *Nippon Kagaku Kaishi* **1992**, *7*, 745.
8. Huang, Z. H.; Kang, F. Y.; Liang, K. M. *Proceedings of 1st World Conference on Carbon*; Berlin: German Carbon Group, 2000, 143.
9. Tang, M. M.; Bacon, R. *Carbon* **1964**, *2*(1), 211.
10. Arons, G. N.; Macnair, R. N. *Textile Research Journal* **1972**, *42*(1), 60.
11. Arons, G. N.; Macnair, R. N. *Textile Research Journal* **1975**, *45*(1), 91.
12. Daguerrea, E.; Stoeckli, G. *Carbon* **2001**, *39*, 1279.
13. Yulia, V.; Basova, V.; Edie, D. D.; Lee, Y.; Laura, K.; Ryu, S. K. *Carbon* **2004**, *42*, 485.
14. Rodrýguez-Reinoso, F.; Pastor, A. C.; Marsh, H.; Martýnez, M. A. *Carbon* **2000**, *38*, 379.
15. Rosas, J. M.; Bedia, J.; Rodriguez-Mirasol, J.; Cordero, T. *Fuel* **2009**, *88*, 19.
16. Valente, J. M. *et al. J. Porous Mat.* **2007**, *14*, 181. DOI 10.1007/s10934-006-9023-0.
17. Vicente, J.; Paula, S.; Luis jose, V.; Romero, A. *Materials Chemistry and Physics* **2010**, *124*(1), 223.
18. Young, C. B.; Wang, K. *et al. Korean Chemical Engineering Research* **2005**, *43*, 146.
19. Gergova, K.; Galushko, A.; Petrov & Minkova, N. *Carbon* **1992**, *30*(5), 721.
20. Rosas, J. M.; Bedia, J.; Rodriguez-Mirasol, J.; Cordero, T. *Fuel* **2009**, *88*, 19.
21. Eduardo, M.; Correa, C.; Angeles, M.; Angel, L. *Microporous and Mesoporous Materials* **2008**, *111*, 523.
22. Su, C.-I.; Wang, C.-L. *Fibers and Polymers* **2007**, *8*(5), 477.
23. Kyotoni, T. *Control of Pore Structure of Carbon*; *Carbon* **2000**, *38*, 269.